International Journal of Bifurcation and Chaos, Vol. 13, No. 11 (2003) 3235–3253

PSEUDO-DETERMINISTIC CHAOTIC SYSTEMS

R. L. VIANA, S. E. DE S. PINTO and J. R. R. BARBOSA*
Departamento de Física, Universidade Federal do Paraná,
Caixa Postal 19081, 81531-990, Curitiba, Paraná, Brasil

C. GREBOGI
Instituto de Física, Universidade de São Paulo,
Caixa Postal 66318, 05315-970, São Paulo, São Paulo, Brasil

Received December 12, 2002; Revised February 3, 2003

We call a chaotic dynamical system pseudo-deterministic when it does not produce numerical, or pseudo-trajectories that stay close, or shadow chaotic true trajectories, even though the model equations are strictly deterministic. In this case, single chaotic trajectories may not be meaningful, and only statistical predictions, at best, could be drawn on the model, like in a stochastic system. The dynamical reason for this behavior is nonhyperbolicity characterized either by tangencies of stable and unstable manifolds or by the presence of periodic orbits embedded in a chaotic invariant set with a different number of unstable directions. We emphasize herewith the latter by studying a low-dimensional discrete-time model in which the phenomenon appears due to a saddle-repeller bifurcation. We also investigate the behavior of the finite-time Lyapunov exponents for the system, which quantifies this type of nonhyperbolicity as a system parameter evolves past a critical value. We argue that the effect of unstable dimension variability is more intense when the invariant chaotic set of the system loses transversal stability through a blowout bifurcation.

Keywords: Chaotic systems; hyperbolic systems; shadowing; Lyapunov.

1. Introduction

(. . .) *"We conclude this discussion by mentioning what seems to be an interesting issue*: *the loss of hyperbolicity due to the existence of fixed points embedded in the attractor that have a number of unstable directions* (*that is*, *eigenvalues with magnitude bigger than one*) *different from the number of unstable directions of the attractor* (*that is*, *positive Lyapunov exponents*)*"* (quoted from [Romeiras *et al.*, 1992]).

The extreme sensitiveness to initial conditions displayed by chaotic systems often leads to a puzzling question: should we believe the numerical chaotic trajectories obtained when using a computer? Are these trajectories "real", in the sense that they emulate actual chaotic orbits of the system? If so, to what extent can we assess the goodness of the numerical trajectories [Grebogi *et al.*, 1990]? The answers to these questions are, to a large extent, within the realm of shadowability theory [Grebogi *et al.*, 1987, 1988a]. Loosely speaking, a numerically generated chaotic trajectory is said to shadow a "true" chaotic trajectory if the former stays uniformly close to the latter and *vice versa* [Grebogi *et al.*, 2002]. The shadowing of numerical trajectories, for a reasonable timespan, is a minimum requirement for a meaningful computer simulation of a physical process. This obviously

*Permanent Address: Departamento de Matemática, Universidade Federal do Paraná, 81531-990, Curitiba, PR, Brasil.

does not preclude other equally important prerequisites of a more epistemological nature, like the validity of the model proposed for describing the physical phenomenon, or the correctness of the assumptions on which the model is based. However, the shadowability requirement for a chaotic trajectory is one of the most difficult to be fulfilled since it is strongly based on the hyperbolicity of the dynamics [Sauer & Yorke, 1991].

Most dynamical systems of physical, biological and technological interest are not hyperbolic, so the lack of shadowability seems to haunt the credibility of numerical simulations of chaotic processes used by scientists and engineers in their activities. In this paper, we deal with the limits of shadowability theory, investigating chaotic dynamical systems whose numerical trajectories do not typically have the shadowing property, i.e. the existence of true trajectories in their neighborhood. Hence these trajectories are not meaningful if taken only by themselves, although, sometimes, valid conclusions could be drawn based on a statistical treatment from assemblies of such trajectories, like averages and fluctuations [Lai *et al.*, 1999a; Sauer, 2002]. So, they could yield at best the same kind of information expected from a stochastic system, in spite of the fact that the dynamical system trajectories are governed by strictly deterministic model equations. This is the reason we are calling them *pseudo-deterministic* [Viana & Grebogi, 2000].

The breakdown of shadowability for a pseudo-deterministic dynamical system occurs in a rather strong way, in the sense that the time a computer-generated trajectory stays close to an actual chaotic one is too short for most applications. From the mathematical point of view, this severe breakdown of shadowability stems from a strong form of nonhyperbolicity, that has been called *unstable dimension variability*, or UDV for short [Romeiras *et al.*, 1992; Dawson *et al.*, 1994]. In this case, unstable periodic orbits embedded in a chaotic invariant set, such as a chaotic attractor, have different numbers of unstable directions. For a discrete-time map, this means that the number of eigenvalues with moduli greater than unity is different for periodic orbits in the chaotic invariant set. This violates the continuous splitting between stable and unstable directions along a trajectory, which is a fundamental property of hyperbolic sets [Guckenheimer & Holmes, 1983]. Since the sets of points with different unstable dimensions are, apparently, densely interwoven in a chaotic invariant set, UDV leads to a shadowability breakdown [Lai & Grebogi, 2000a].

Although it may seem at first that UDV is nothing but a mathematical pathology, unlikely to be found in real dynamical systems, it turns out that it has been identified in many models of physically interesting situations [Dawson *et al.*, 1994]. In particular, there is numerical evidence and theoretical arguments showing that coupled chains of oscillators exhibit UDV for a wide range of coupling strengths [Lai *et al.*, 1999b]. This should call the attention of applied scientists or engineers for the potentially crucial questions related to the shadowability properties of the model that they are numerically investigating. The main goal of this paper is to survey the fundamental results, as well as to present a detailed study of a case example in which UDV has been shown analytically and numerically to occur. Throughout the text, we refer to the pertinent literature for more precise statements as well as for the technical details of the proofs [Grebogi *et al.*, 2002].

The rest of this paper is organized as follows: in Sec. 2 we present some basic definitions, emphasizing the concepts of hyperbolicity of invariant sets. Section 3 aims to present basic ideas in shadowability theory. Section 4 is devoted to a discussion of UDV, and Sec. 5 works out a case study in which UDV occurs in a two-dimensional map with an invariant subspace. Numerical procedures to detect and quantify UDV are described in Sec. 6. Section 7 treats a kind of intermittent chaotic bursting induced by UDV. The last section contains our conclusions.

2. Basic Definitions

We shall outline some basic definitions which are used throughout the paper. Discrete time mappings are chosen, bearing in mind that continuous time flows may also be described by them, if they are invertible, using Poincaré sections. Let $\mathbf{f} : \mathcal{R}^m \to \mathcal{R}^m$ be a diffeomorphism $\mathbf{x} \mapsto \mathbf{f}(\mathbf{x})$, $x \in \mathcal{R}^m$, possessing an invariant set Ω, such that if $\mathbf{x} \in \Omega$, any subsequent forward or backward iterate of $\mathbf{x}$ remains in Ω. The invariant set Ω is called hyperbolic if the tangent space at a point $\mathbf{x}$ of Ω, denoted as $T_{\mathbf{x}}$, may be decomposed as the direct sum [Guckenheimer & Holmes, 1983]

$$T_{\mathbf{x}} = E^u_{\mathbf{x}} \oplus E^s_{\mathbf{x}}\,, \tag{1}$$

where $E^u_{\mathbf{x}}$ and $E^s_{\mathbf{x}}$ are the unstable and stable subspaces, respectively, having the following properties:

(i) The decomposition (1) varies *continuously* with $\mathbf{x} \in \Omega$, and it is invariant under the action of the tangent map such that the unstable and stable subspaces are consistent under the dynamics of the tangent map $\mathbf{Df}$.

$$\mathbf{Df}(E^u_{\mathbf{x}}) = E^u_{\mathbf{f(x)}}\,, \tag{2}$$

$$\mathbf{Df}(E^s_{\mathbf{x}}) = E^s_{\mathbf{f(x)}}\,; \tag{3}$$

(ii) There exist constants $K > 0$ and $0 < \rho < 1$, such that

$$\|\mathbf{Df}^n(\mathbf{x})\mathbf{y}\| < K\rho^n\|\mathbf{y}\| \quad \text{if} \quad \mathbf{y} \in E^s_{\mathbf{x}}\,, \tag{4}$$

$$\|\mathbf{Df}^{-n}(\mathbf{x})\mathbf{y}\| < K\rho^n\|\mathbf{y}\| \quad \text{if} \quad \mathbf{y} \in E^u_{\mathbf{x}}\,, \tag{5}$$

meaning that vectors in a small neighborhood of $E^s_{\mathbf{x}}$ ($E^u_{\mathbf{x}}$), under the forward (backward) iterations of the tangent map $\mathbf{Df}$, approach any $\mathbf{x} \in \Omega$ at a uniform rate ρ.

The *stable* (*unstable*) *dimension* at a point $\mathbf{x} \in \Omega$ is the dimension of the corresponding stable (unstable) subspace $d^s = \dim E^s_{\mathbf{x}}$ ($d^u = \dim E^u_{\mathbf{x}}$). Since $\mathbf{f(x)}$ is a diffeomorphism, $\mathbf{Df(x)}$ is an isomorphism, and $\dim E^{u,s}_{\mathbf{x}} = \dim E^{u,s}_{\mathbf{f(x)}}$, i.e. the stable and unstable dimensions do not change along a trajectory belonging to a hyperbolic set Ω. For this invariant set Ω of the nonlinear map $\mathbf{f(x)}$, the stable, $W^s(\mathbf{x})$, and the unstable, $W^u(\mathbf{x})$, manifolds of the fixed point $\mathbf{x} \in \Omega$ are defined as [Devaney, 1989]:

$$W^s(\mathbf{x}) = \{\mathbf{y} \in \mathcal{R}^m : \mathbf{f}^n(\mathbf{y}) \to \mathbf{x} \ \text{ if } \ n \to \infty\}\,, \tag{6}$$

$$W^u(\mathbf{x}) = \{\mathbf{y} \in \mathcal{R}^m : \mathbf{f}^{-n}(\mathbf{y}) \to \mathbf{x} \ \text{ if } \ n \to \infty\}\,, \tag{7}$$

respectively.

Due to the local manifold theorem [Wiggins, 1990] for a hyperbolic C^r-diffeomorphism, there exist stable and unstable invariant manifolds, and they are tangent to the stable and unstable invariant subspaces of the tangent map $\mathbf{Df(x)}$ at the fixed points $\mathbf{x}$ embedded in Ω. Moreover, in hyperbolic systems the unstable and stable manifolds must intersect transversely, i.e. the angle between them is bounded away from zero. As a consequence, homoclinic or heteroclinic tangencies between the manifolds break the hyperbolicity of the invariant set Ω [Grebogi *et al.*, 1983]. There has been also recognized the *structural stability* of hyperbolic sets: the dynamics on them is topologically the same under small bounded perturbations of the map $\mathbf{f(x)}$ [Palis & de Melo, 1982].

The existence of bifurcations in the dynamics, as a system parameter is varied, restricts the applicability of the hyperbolicity concept to a few cases, like axiom-A systems [Ruelle, 1989]. Most dynamical systems of physical and technological interest are nonhyperbolic, most likely due to the existence of homoclinic tangencies, but also because of a failing in the continuous direct-sum splitting (1) between stable and unstable subspaces in every point of the invariant set. The latter is the key issue addressed in this paper.

3. Shadowing Theory in a Nutshell

An interesting numerical experiment that can be made using the Hénon map $(x, y) \mapsto (1 - 1.4x^2 + y, 0.3x)$ (which has a chaotic attractor [Benedicks & Carleson, 1991]) is the computation of the first hundred iterates from an initial condition, say $(0, 0)$, by using both single and double precision accuracies, the difference in accuracy being of the order 10^{-14} [Gulick, 1990]. It turns out that in less than 50 iterates, the trajectories obtained from single and double precision accuracy are far apart at a distance comparable to the size of the chaotic attractor. How can one trust the validity of such computer-generated trajectories?

The results of shadowing theory [Grebogi *et al.*, 1990; Anosov, 1967; Bowen, 1975; Katok & Hasselblatt, 1995] guide us to assess the validity of chaotic trajectories in face of dynamical difficulties arising from the breaking of hyperbolicity. If there is continuous shadowability of trajectories, even though a computer-generated trajectory may eventually depart with time from a "true" chaotic trajectory which is the goal of the simulation, there exists another fiducial trajectory that shadows, or "stays close to", the computer-generated trajectory for the time-span of interest. This "true" chaotic orbit may not be the one we have sought for, since it will start from a generally different initial condition, but this fact does not matter for many applications. These shadowing orbits are thus reliable for, say, computations of long-time averages such as entropies and dimensions [Grassberger *et al.*, 1989].

3.1. *Definitions*

In what follows, we will cast these heuristic arguments in a more formal context. Let $\mathbf{f} : \mathcal{R}^m \to \mathcal{R}^m$ be a diffeomorphism, that may also represent a

Poincaré time-T map of a nonautonomous flow. Suppose that $\mathbf{z}_0 \in \mathcal{R}^m$ represents the current state of the system, thus $\mathbf{f}(\mathbf{z}_0)$ is the "true" state after a time T [Poon *et al.*, 1994]. If this map comes, for example, from the numerical integration of some system of first-order ordinary differential equations, we have to use some numerical integrator like the Runge–Kutta or Bulirsch–Stoer methods. There are basically two sources of numerical error in such a procedure: (i) the time discretization process itself; and (ii) the finite-precision accuracy due to roundoff errors.

Both kinds of errors can be reduced but not eliminated at all, generating a discrepancy between the numerical result, which we denote $\mathbf{z}_1$, and the expected or "true" state $\mathbf{f}(\mathbf{z}_0)$ after a time T. The characteristic error is usually bounded so that $\|\mathbf{z}_1 - \mathbf{f}(\mathbf{z}_0)\| < \delta$, where $\delta > 0$ is supposed to be a small number, and $\|\cdots\|$ stands for the Euclidean norm in $\mathcal{R}^m$. In this case we say that $\mathbf{z}_0$ and $\mathbf{z}_1$ are points of a δ-pseudo-trajectory of the map $\mathbf{f}$. In general, $\{\mathbf{z}_n\}_{n=0}^N = \{\mathbf{z}_0, \mathbf{z}_1, \ldots \mathbf{z}_N\}$, are points of a δ-pseudo-trajectory if [Grebogi *et al.*, 1988a] $\|\mathbf{z}_{n+1} - \mathbf{f}(\mathbf{z}_n)\| < \delta$, for $n = 0, 1, \ldots, N-1$.

On the other hand, leaving aside for a moment the issue of numerical integration, the existence theorem for differential equations [Arnold, 1978; Guckenheimer & Holmes, 1983] warrants that there exists a "true" chaotic trajectory of length $N+1$ for the map $\mathbf{f}$ comprising of the points $\{\mathbf{x}_n\}_{n=0}^N = \{\mathbf{x}_0, \mathbf{x}_1, \ldots \mathbf{x}_N\}$, such that $\mathbf{x}_{n+1} = \mathbf{f}(\mathbf{x}_n)$, $n = 0, 1, \ldots, N-1$. We say that a "true" trajectory $\{\mathbf{x}_n\}_{n=0}^N$ ε-shadows a δ-pseudo trajectory $\{\mathbf{z}_n\}_{n=0}^N$ if there is a $\varepsilon > 0$ such that [Grebogi *et al.*, 2002] $\|\mathbf{x}_n - \mathbf{z}_n\| < \varepsilon$, for $n = 0, 1, \ldots, N-1$.

Let $\mathbf{Z} = \{\mathbf{z}_0, \ldots, \mathbf{z}_N\}$ be a pseudo-trajectory and $\mathbf{E} = \{\mathbf{z}_1 - \mathbf{f}(\mathbf{z}_0), \ldots, \mathbf{z}_N - \mathbf{f}(\mathbf{z}_{N-1})\}$ be the related error vector. A "true" trajectory $\mathbf{X} = \{\mathbf{x}_0, \ldots, \mathbf{x}_N\}$ is then related to the null error vector $\mathbf{0}$. If we can continuously deform the pseudo-trajectory to the true one, there exists an error function $\mathbf{F} : \mathbf{Z} \to \mathbf{E}$, such that $\mathbf{F}^{-1}(\mathbf{E})$ goes from $\mathbf{Z}$ to $\mathbf{X}$ continuously as $\mathbf{E}$ goes to $\mathbf{0}$. In this case the pseudo-trajectory $\mathbf{Z} = \{\mathbf{z}_0, \ldots, \mathbf{z}_N\}$ is said to be *continuously-shadowable* [Poon *et al.*, 1994].

A direct numerical method to test these conditions for shadowability uses the concept of *brittleness*, which is, for a pseudo-trajectory, the ratio between the shadowing distance and the one-step error due to computer roundoff and/or truncation procedure $\mathcal{B} = \max_n(\|\mathbf{z}_n - \mathbf{x}_n\|/\delta)$, and a necessary condition for continuous shadowability is that the product of the brittleness and the magnitude of the error vector $\mathbf{E}$ of the pseudo-trajectory be smaller than the attractor size [Grebogi *et al.*, 1990, 2002] .

3.2. *Shadowing in hyperbolic and nonhyperbolic systems*

Anosov [1967] and Bowen [1975] proved that, for hyperbolic systems like axiom-A diffeomorphisms [Ruelle, 1989], pseudo-trajectories are continuously shadowable for an infinite time, i.e. there exists a $\delta > 0$ such that all δ-pseudo-trajectories $\{\mathbf{z}_n\}_{n=0}^N$ in an invariant hyperbolic set Ω are ε-shadowable by a "true" trajectory $\{\mathbf{x}_n\}_{n=0}^N$ for arbitrarily long times. Let us present a short outline of the proof of the shadowability lemma [Meyer & Hall, 1992; Grebogi *et al.*, 2002], in order to highlight where the hyperbolicity requirement enters in the reasoning leading to continuous shadowability.

Let $\mathbf{Z}_\infty = \{\ldots \mathbf{z}_{-1}, \mathbf{z}_0, \mathbf{z}_1, \ldots\}$ be a shadowing δ-pseudo-trajectory of arbitrary length, and V be the space of these vectors of infinite length, with a suitable norm $\|\mathbf{Z}_\infty\| = \sup_n |\mathbf{z}_n|$. We define a function $\mathcal{G} : V \to V$ such that $(\mathcal{G}(\mathbf{Z}_\infty))_n = \mathbf{f}((\mathbf{Z}_\infty)_{n-1}) = \mathbf{f}(\mathbf{z}_{n-1})$, where $\mathbf{f}$ is supposed to be a smooth hyperbolic map, and $(.)_i$ denotes the ith component of a vector in V. If $\mathbf{X}_\infty$ is a fixed point of $\mathcal{G}$, then $\mathbf{X}_\infty$ is a true trajectory since $(\mathcal{G}(\mathbf{X}_\infty))_n = \mathbf{x}_n = \mathbf{f}(\mathbf{x}_{n-1})$.

From the previous definition, $\mathbf{Z}_\infty$ is a δ-pseudo-trajectory if $\|\mathcal{G}(\mathbf{Z}_\infty) - \mathbf{Z}_\infty\| < \delta$. Defining $\mathcal{F}(\mathbf{Z}_\infty) = \mathcal{G}(\mathbf{Z}_\infty) - \mathbf{Z}_\infty \equiv \mathbf{E}_\infty$, we can cast the shadowability lemma in the following form: for every $\varepsilon > 0$, there exists a $\delta > 0$ such that if $\|\mathcal{F}(\mathbf{Z}_\infty)\| = \|\mathbf{E}_\infty - \mathbf{0}\| < \delta$, then there is a fixed point $\mathbf{X}_\infty$ of $\mathcal{G}$ such that $\|\mathbf{Z}_\infty - \mathbf{X}_\infty\| = \|\mathcal{F}^{-1}(\mathbf{E}_\infty) - \mathcal{F}^{-1}(\mathbf{0})\| < \varepsilon$, and $\mathcal{F}$ and $\mathbf{E}_\infty$ may be regarded as extensions of the function $\mathbf{F}$ and the error vector $\mathbf{E}$, respectively.

The requirement of $\mathbf{f}$ being a smooth map with a hyperbolic structure, Eqs. (2)–(4), is necessary to shown that the jacobian derivative $D\mathcal{F}$ and its inverse $D\mathcal{F}^{-1}$ are both bounded in the linear vector space to which V belongs. Let $B_\eta(\mathbf{Z}_\infty)$ denote a ball (in the vector space V) of radius η centered at the point $\mathbf{Z}_\infty$. The implicit function theorem thus guarantees the existence of a domain Λ, with $B_\rho(\mathbf{Z}_\infty) < \Lambda < B_\eta(\mathbf{Z}_\infty)$, such that $\mathcal{F}$ is one-to-one on Λ, and $B_\sigma(\mathcal{F}(\mathbf{Z}_\infty)) = B_\sigma(\mathbf{E}_\infty) \subset \mathcal{F}(\Lambda)$. A proper choice of η would imply $\mathbf{0} \in B_\eta(\mathbf{E}_\infty)$, and there is a unique true trajectory $\mathbf{X}_\infty \in \Lambda$ such that $\mathcal{F}(\mathbf{X}_\infty) = \mathbf{0}$. Moreover, we have $\|\mathbf{Z}_\infty - \mathbf{X}_\infty\| <$

$\eta \leq \varepsilon$, so that we have an ε-shadowing trajectory. The implicit function theorem ensures the continuity of $\mathcal{F}^{-1}$ on $B_\sigma(\mathbf{E}_\infty)$, meaning that all pseudo-trajectories (including $\mathbf{Z}_\infty$) in a small neighborhood of $\mathbf{X}_\infty$ are continuously shadowed by the same true trajectory $\mathbf{X}_\infty$.

However, as we have mentioned in the previous section, the hyperbolicity requirement is too strong for most dynamical systems of physical and technological interest. Moreover, even if the invariant set is hyperbolic but has a fractal measure (with respect to the Lebesgue measure) the shadowability lemma may not be applicable since there is no reason for the pseudo-trajectory to lie in the invariant set [Poon *et al.*, 1994]. Even a robustly transitive diffeomorphism having a strong partially hyperbolic splitting for the tangent space $T_{\mathbf{x}} = E^u_{\mathbf{x}} \oplus E^s_{\mathbf{x}} \oplus E^c_{\mathbf{x}}$ (in which there exists also a central invariant subspace) fails to obey the shadowability lemma [Bonatti *et al.*, 2000].

The applicability of the shadowability theory to nonhyperbolic system was extensively investigated in the late 80's [Grebogi *et al.*, 1987, 1988a, 1990]. When a system fails to be hyperbolic due to homoclinic tangencies, it was proved that pseudo-trajectories can still be continuously shadowable for a long, but finite time. The proof is technically involved, but states basically that if certain quantities calculated at the points of a pseudo-trajectory are bounded, then there exists a "true" trajectory close to the pseudo-trajectory. Another way to express this result is that, for nearly hyperbolic systems, locally sensitive trajectories are often globally insensitive [Sauer, 2002]. For each point of the pseudo-trajectory, subspaces complementary to the tangent space are defined such that they can approach the stable and unstable manifolds provided these complementary subspaces exist. Hence, pseudo-trajectories may be continuously shadowable for a finite time-span. Failures of continuous shadowability of pseudo-trajectories are called *glitches*, and may be due to near-tangencies between invariant manifolds [Grebogi *et al.*, 2002]. The time we are able to verify continuous shadowability in this case is basically the time interval until a pseudo-trajectory encounters a glitch. Since numerical results use finite-time pseudo-trajectories, these may have the adequate shadowability properties. These claims have been confirmed by carefully designed numerical experiments [Dawson *et al.*, 1994].

3.3. *Model shadowability*

We can think of a pseudo-trajectory in two equivalent ways. One is to suppose, as we have done here, that it comes from the numerical integration of an "exact" model, a process that introduces unavoidable roundoff errors that make the computer-generated trajectory to exponentially diverge from the "true" chaotic trajectory. An equivalent point of view is that the pseudo-trajectory results from an imperfect model, which is a slightly perturbed version of the "exact" model [Lai *et al.*, 1999a; Lai & Grebogi, 2000a]. The small difference between two mathematical models, denoted as $\mathcal{A}$ and $\mathcal{B}$, of a same physical process can be due to several factors: (i) small differences in the parameter values of the models; (ii) small deviations on the external influence (as a periodic driving term) on each model; or (iii) a small bounded noise level in either model (what excludes an unbounded Gaussian noise, for example).

Successful mathematical modeling requires that the set of all possible results from model $\mathcal{A}$ agree, in an approximate way, with all possible results from model $\mathcal{B}$ (*model shadowability* [Lai *et al.*, 1999a; Lai & Grebogi, 2000a]). $\mathcal{A}$ and $\mathcal{B}$ are said to exhibit model shadowability if each trajectory obtained from model $\mathcal{A}$ is continuously shadowed by some trajectory obtained from model $\mathcal{B}$. This turns out to be a necessary condition for either model to properly describe the dynamical behavior of the physical phenomenon being investigated. If the models fail to exhibit this property, it is claimed that no trajectory of $\mathcal{A}$ can be continuously shadowed by trajectories of $\mathcal{B}$. Hence it is unlikely that either model could produce chaotic trajectories realized by Nature.

The applicability of the shadowability properties for typical trajectories of nonhyperbolic systems presenting homoclinic tangencies enables us to extend the model shadowability concept to such systems. As an illustrative example, let $\mathcal{A}$ be the Hénon map, with a nonhyperbolic chaotic attractor, due to the infinite number of tangencies between stable and unstable manifolds of the embedded unstable periodic orbits [Grebogi *et al.*, 1983]. Model $\mathcal{B}$ could be a noisy version of $\mathcal{A}$, in which a term ϖd_n, where $\varpi \ll 1$ and d_n is a zero-mean bounded noise with a uniform distribution in $[0, 1]$, added to the x-part of the map. Chaotic trajectories of the noisy Hénon map $\mathcal{B}$ can be continuously shadowed by trajectories of the original map $\mathcal{A}$ up to a time $\varpi^{-\alpha}$, where $\alpha \lesssim 1/2$ is the scaling exponent [Grebogi

et al., 1987, 1988a]. This is basically the average time interval it takes for a pseudo-trajectory to fall in the neighborhood of an homoclinic tangency, or a glitch.

4. Unstable Dimension Variability

UDV is a property of unstable periodic orbits embedded in a chaotic invariant set having a different number of unstable eigendirections, i.e. the unstable dimension d^u is not constant for points belonging to Ω. Such chaotic invariant sets are strongly nonhyperbolic, because the subspaces $E^u_{\mathbf{x}}$ and $E^s_{\mathbf{x}}$ are not invariant along a typical chaotic trajectory.

As an illustrative example, let $\mathbf{f}$ be a two-dimensional map with an invariant chaotic (nonattracting) set Ω with an infinite number of embedded unstable fixed points. Now suppose that a fraction of these points are saddles (one stable and one unstable direction) and the remaining are repellers (two unstable directions). Consider a typical chaotic trajectory on this invariant set Ω. As it evolves in time, the trajectory visits the neighborhood of an infinite number of saddles and repellers, due to the ergodicity of the dynamics on Ω. If we take a small disk of initial conditions near a saddle, it will shrink along the stable manifold and elongate along the unstable manifold, becoming a thin filament. While this occurs, it is still possible to shadow orbits within the filament, since the dynamics is hyperbolic then. However, points belonging to this filament will eventually approach repellers, and they will diverge from perturbed trajectories due to the new unstable direction. The result is the lack of continuous shadowability of typical trajectories after a relatively short timespan. This limits, in a severe way, the usefulness of such systems in situations for which the timescale of interest is higher than the time for which shadowing applies.

UDV has been first described by Abraham and Smale [1970] for a diffeomorphism in $T^2 \times S^2$ whose invariant set has two fixed points with different unstable dimensions. However, the first observation of UDV for a dynamical system of physical interest did not appear until 1992, when its existence was incidentally reported for the impulsively kicked double rotor, described by the following four-dimensional invertible map [Romeiras *et al.*, 1992]

$$\begin{pmatrix} \mathbf{X} \\ \mathbf{Y} \end{pmatrix} \mapsto \begin{pmatrix} \mathbf{X}' \\ \mathbf{Y}' \end{pmatrix} = \begin{pmatrix} \mathbf{M}\mathbf{Y} + \mathbf{X} \\ \mathbf{L}\mathbf{Y} + \mathbf{G}(\mathbf{X}') \end{pmatrix} \qquad (8)$$

where $\mathbf{X} = (x_1, x_2)^T \in S^1 \times S^1$, are the angular positions of the rotor rods at discrete times nT ($n \in \mathcal{Z}$), T being the period of the delta-function excitation, and $\mathbf{Y} = (y_1, y_2)^T \in R^2$, the corresponding angular velocities just after each delta kick. The nonlinear functions are $\mathbf{G}(\mathbf{X}') = (c_1 \sin x'_1, c_2 \sin x'_2)^T$, where c_i are functions of the kick strength f_0 (which is the control parameter of the system). $\mathbf{L}$ and $\mathbf{M}$ are 2×2 constant matrices whose entries are functions of the remaining physical parameters of the rotor, including the dissipation coefficients.

Due to the $y_i \to -y_i$ symmetry of the kicked double rotor map, it turns out that the plane $y_1 = y_2 = 0$ is an invariant subspace of the system, such that four of its fixed points lie on this subspace and can be classified in one-parameter families $(\mathbf{X}^*, \mathbf{Y}^*)^T = (x_1^{(n_1,n_2,q)}, x_2^{(n_1,n_2,q)}, 0, 0)^T$, where $n_1 = n_2 = 0$ are integer rotation numbers, and $q = 1, 2, 3, 4$. Let us focus our attention on the unstable fixed point P, for which $x_1^* = x_2^* = \pi$. For $f_0 \lesssim f_{0C} \approx 8.1104126$ it has three stable eigendirections and one unstable eigendirection, i.e. $d^u = 1$. At $f_0 = f_{0C}$ there is a period-doubling bifurcation (eigenvalue $= -1$) such that, for $f_0 \gtrsim f_{0C}$ the point P has now two stable and two unstable eigendirections ($d^u = 2$). Every preimage of P shares the same property. We remark that $(\pi, \pi, 0, 0)$ is a stable period-1 orbit which undergoes a period-doubling bifurcation at lower value of f_0, namely ≈ 4.27, which is followed by a period-doubling cascade which accumulates at $f_0 \approx 6.75$.

Hence, after this bifurcation there is an infinite number of fixed points embedded in the chaotic attractor with either one or two unstable directions, which identifies the occurrence of UDV at $f = f_{0C}$. It was recognized that this is related to the fluctuating behavior (around zero) of the finite-time Lyapunov exponent closest to zero [Dawson *et al.*, 1994]. If the latter fluctuates about zero during a trajectory, we have a tangential direction which is uncertain between expansion and contraction [Sauer, 2002]. The brittleness of numerical pseudo-trajectories of the double rotor, when it exhibits UDV, has been shown to increase to very high values [Grebogi *et al.*, 2002].

In the case of the kicked double rotor, the invariant set of interest is a chaotic attractor, but UDV can also appear in nonattracting chaotic sets, as strange saddles smooth along an unstable direction [Dawson, 1996]. A map on the 2-torus,

with dense sets of saddles and repellers, was found to exhibit UDV by Kostelich *et al.* [1997]. The presence of UDV seems to be typical in general high-dimensional dynamical systems, as shown by Lai and Grebogi [1999a], who have described its occurrence in globally coupled Hénon and Ikeda map lattices.

The latter observation can be put in a more general context, if one considers the problem of modeling coupled chaotic oscillators. Since the seminal work of Pecora and Carroll [1990] it has been recognized that an array of chaotic oscillators can synchronize their trajectories. For a general class of coupled map lattices

$$\mathbf{x}_{n+1}^{(i)} = \mathbf{F}(\mathbf{x}_n^{(i)}) - \frac{\varepsilon}{2}\sum_{j=1}^{N} g_{ij}\mathbf{H}(\mathbf{x}_n^{(j)})\,, \quad (i = 1, 2, \ldots, N)\,, \tag{9}$$

or coupled oscillator chains,

$$\frac{d\mathbf{x}^{(i)}(t)}{dt} = \mathbf{F}(\mathbf{x}^{(i)}(t)) - \frac{\varepsilon}{2}\sum_{j=1}^{N} g_{ij}\mathbf{H}(\mathbf{x}^{(j)}(t))\,, \quad (i = 1, 2, \ldots, N)\,, \tag{10}$$

where $\mathbf{x}^{(i)} \in \mathcal{R}^D$ and $\mathbf{F}$, $\mathbf{H}$ are D-dimensional smooth vector functions, it turns out that the synchronization manifold

$$\mathbf{x}^{(1)} = \mathbf{x}^{(2)} = \cdots = \mathbf{x}^{(N)} \tag{11}$$

is a chaotic invariant set for the system (9), provided $\sum_j g_{ij} = 0$ [Lai & Grebogi, 1999].

UDV has been numerically observed in a system of locally coupled Hénon maps in the form as Eq. (9) *for any nonzero* coupling strength ε [Lai & Grebogi, 2000a]. The coupled maps may also be regarded as Poincaré maps of continuous time flows. In fact, systems of continuous-time oscillators coupled in the form (10) have also been argued to exhibit UDV, as it was numerically confirmed for chains of Rössler oscillators [Lai *et al.*, 1999b]. Not only the completely synchronized state (11), but also phase synchronized states in chaotic systems were proved to exhibit UDV for nonvanishing coupling strength [Andrade & Lai, 2001].

The ubiquitous presence of UDV in chaotic systems with invariant subspaces is expected on rather general grounds [Lai, 1996; Lai & Grebogi, 2000a], since the number of unstable directions of any unstable periodic orbit embedded in the invariant chaotic set is determined by: (i) the local chaotic dynamics on the invariant subspace; and (ii) the transverse dynamics [such as the coupling strength in Eq. (9)]. In particular, the appearance of UDV in the synchronization manifold of coupled chaotic oscillators is related to the so-called *bubbling transition*, in which periodic orbits embedded in the manifold lose transversal stability [Ashwin *et al.*, 1994, 1996].

If the interacting systems are not identical, or if they are very weakly coupled, they do not present in general exact amplitude synchronization, but they may present a generalized synchrony [Boccaletti *et al.*, 2001]. In this case, instead of a synchronization manifold we focus on an emergent set that arises from a decoherence transition. This mechanism has also been blamed to be a general source of UDV in such systems [Barreto *et al.*, 2000; Barreto & So, 2000]. In high-dimensional systems the transition to hyperchaos, when there are multiple positive Lyapunov exponents, has been also shown to be related to UDV [Davidchack & Lai, 2001]. For dynamical systems possessing two or more asymptotic sets with a different number of unstable directions, extrinsic noise has been shown to lead to UDV [Lai *et al.*, 2003].

It may seem at first that it is hopeless that a chaotic system exhibiting UDV happens to be of practical use, for it would lack adequate shadowability properties. However, if we consider not single trajectories but rather ensembles of them, statistical quantities could sometimes be reliably computed [Lai *et al.*, 1999a; Sauer, 2002]. This was numerically checked by computing the average energy (and its second moment) of a kicked double rotor, by using two slightly different models, and obtaining results which agree within the numerical accuracy [Lai *et al.*, 1999a]. However, there can be found a family of examples exhibiting UDV, for which even tiny one-step errors in numerical simulations cause macroscopic errors (many orders of magnitude higher) in long-term averages [Sauer, 2002]. Another distinctive feature present in systems with UDV is their robustness against external noise [Kantz *et al.*, 2002].

While in complex systems UDV is apparently very common, if not a universal characteristic, the mechanism of its generation is still not completely understood. Hence, in order to investigate this issue, we consider a simple dynamical system that allows for an easier identification of the bifurcation structure underlying the onset of UDV.

5. A Case Study

We consider a class of two-dimensional noninvertible maps with an invariant chaotic set in which embedded unstable orbits can have unstable dimensions equal to either 1 or 2. In particular, the invariant set may be regarded as the synchronization manifold of two coupled one-dimensional maps [Viana & Grebogi, 2000]. On the other hand, the invariant subspace may also appear as a result of some phase-space symmetry of the dynamical system, as it occurs in the kicked double rotor example.

A class of systems with an invariant subspace are the ones with a skew-product structure in the form

$$x_{n+1} = f(x_n)\,, \tag{12}$$

$$y_{n+1} = pg(x_n)y_n + \text{higher order odd powers of } y\,, \tag{13}$$

where $x \in J \subset \mathbf{R}^1$ and $y \in K \subseteq \mathbf{R}^1$. Due to a $y \to -y$ symmetry there is an invariant subspace Σ given by $y = 0$, in such a way that y will be called the transversal direction with respect to Σ. We suppose that $f : J \to J$ is such that there is a chaotic invariant set in $\Omega \subset \Sigma$, and choose $p > 0$ as a bifurcation parameter, satisfying $pg(x_n) \geq 0$ for all $x \in J$. Moreover, we suppose that $g(x) = 1$, when x is some unstable low-period orbit $x = \chi$ in the chaotic set Ω.

A particular example belonging to this family is the following two-dimensional map

$$x_{n+1} = ax_n(1 - x_n)\,, \tag{14}$$

$$y_{n+1} = pe^{-b(x_n-\chi)^2}y_n + y_n^3\,, \tag{15}$$

where $x \in J = [0, 1]$, and we choose a so that there is a dense chaotic orbit on the attractor. There is a positive Lebesgue measure set of values of a for which this is true [Jacobson, 1981]. We set $\chi = 1 - (1/a)$ as an unstable fixed point embedded in the chaotic attractor Ω. This map was introduced to study the formation of riddled basins of attraction [Lai *et al.*, 1996], and exhibits qualitatively different dynamical behaviors according to the value that the bifurcation parameter $p > 0$ takes on.

If $p < 1$ [Fig. 1(a)] there is a fractal boundary between the basin of the chaotic attractor Ω and the basin of the attractor at infinity. The latter arises since there are only *odd* powers of y in the map (15), such that if $|y_n| > 1$, then $|y_{n+1}| > |y_n| > 1$. Once a trajectory off the invariant subspace reaches the $|y| = 1$ line, it asymptotes to infinity. For $p \geqslant 1$ the basin boundary has collided with the attractor, and the latter becomes a nonattracting chaotic saddle [Fig. 1(b)] through a boundary crisis [Grebogi *et al.*, 1983a].

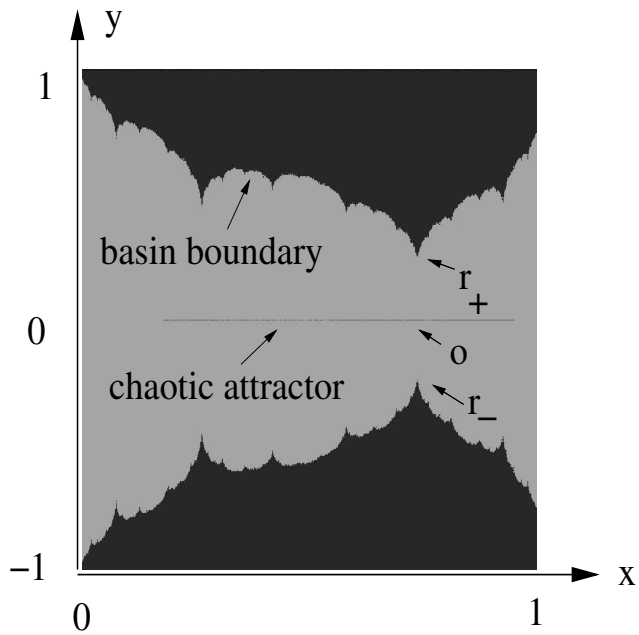

(a)

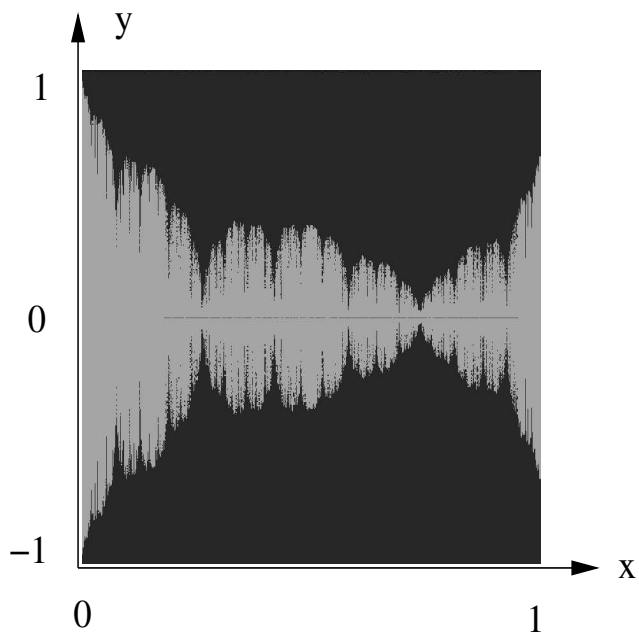

(b)

Fig. 1. Phase portrait of the map (14)–(15) for $a = 3.8$, $b = 5.0$, and: (a) $p = 0.99$; (b) $p = 1.30$. The dark region contains initial conditions that asymptote to infinity, and the gray region is the basin of the attractor at $y = 0$. The arrows indicate the unstable fixed points of the map.

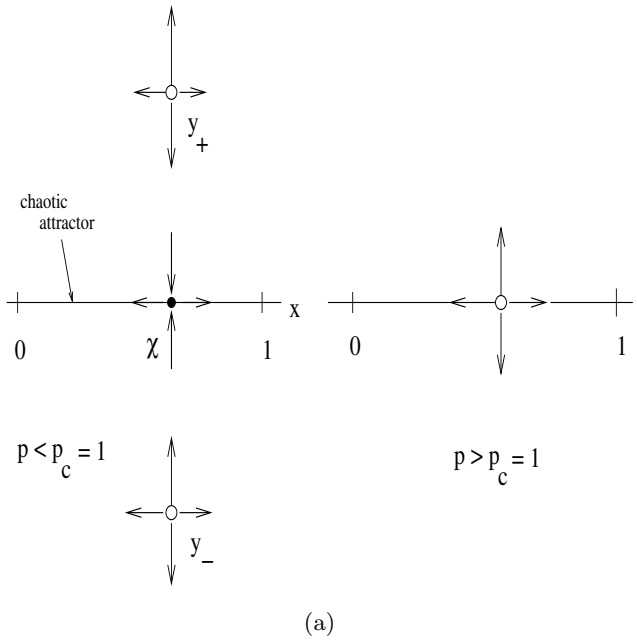

(a)

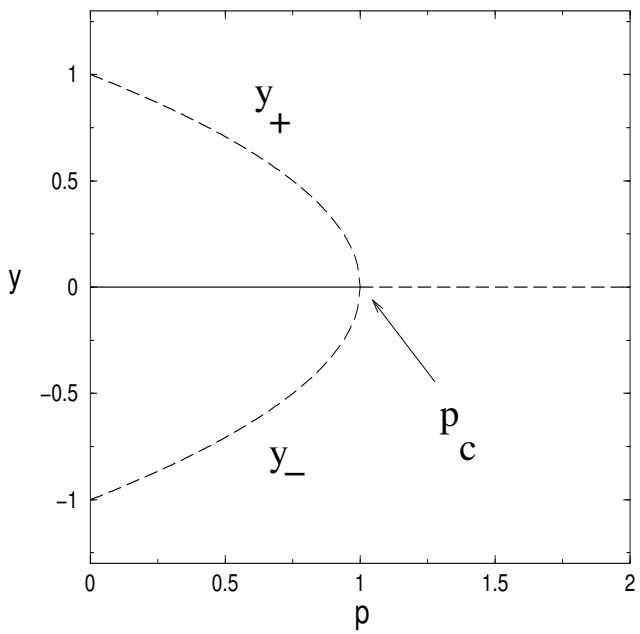

(b)

Fig. 2. (a) Fixed points of the map (14)–(15) before and after the saddle-repeller bifurcation; (b) Bifurcation diagram of (15) at $x = \chi$. Solid (dashed) lines indicate stable (unstable) fixed points.

A linear stability analysis indicates an unstable–unstable pair bifurcation (with eigenvalue $+1$) occurring at $p = p_c = 1$. The fixed points of interest of the map (14–15) are $\mathbf{0} = (\chi, 0)$, and $\mathbf{r}_\pm = (\chi, y^*_\pm = \pm\sqrt{1-p})$ [Fig. 1(a)]. For $p < 1$ (≥ 1) $\mathbf{0}$ is transversely stable (unstable), i.e. $\mathbf{0}$ is a saddle (repeller) with unstable dimension one (two). The

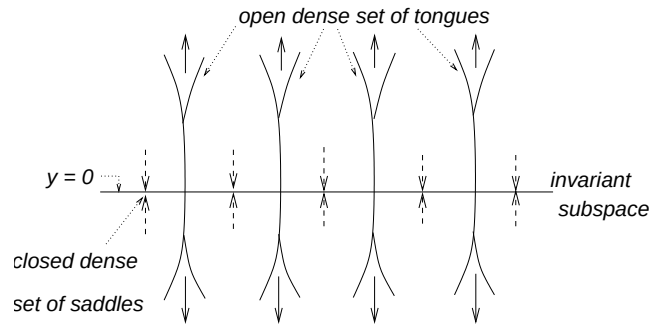

Fig. 3. Schematic figure showing the tongue-like structure that appears for $p > 1$. Adapted from [Lai & Grebogi, 2000b].

other pair of fixed points which we named $\mathbf{r}_\pm$, are located off the invariant subspace [actually they belong to the basin boundaries, cf. Fig. 1(a)] and are repellers for $p < 1$. As p approaches $p_c = 1$, they collide with the fixed point at $y = 0$ and coalesce into a single repeller [Fig. 2(a)]. For all $p \geqslant p_c$ the invariant chaotic set Ω is a nonattracting saddle [Fig. 2(b)].

When the fixed point at $y = 0$ becomes transversely unstable, every preimage of it does so. Since there is a denumerable infinite number of such eventually fixed points embedded in the chaotic set [Gulick, 1990], we conclude that a countably infinite number of periodic saddles become repellers at $p = p_c = 1$, and its complement is a set with an uncountably infinite number of saddles. While the set of newborn repellers has Lebesgue measure zero, the set of saddles has the full Lebesgue measure. Since both sets are dense in Ω, the saddle-repeller (pitchfork) bifurcation at p_c marks the onset of UDV in the system [Viana & Grebogi, 2001].

What is the fate of trajectories off the invariant chaotic set, after this bifurcation has occurred? We already know that, once reaching the $|y| = 1$ line, they asymptote to infinity. However, a feature not revealed by a linear stability analysis, and that stems from the nonlinear terms in Eq. (15), is the existence, between this line and the symmetry plane, of a dense sequence of tongues, anchored at the repellers (Fig. 3). The envelope of these tongues can be analytically estimated [Lai *et al.*, 1996], but their existence can also be inferred from a more general argument, as follows.

Let us consider an open set $\mathcal{O} = |y| > 1$ which intersects the transverse unstable manifold of χ, the repeller belonging to the invariant set Ω. The inverse images of $\mathcal{O}$, which by continuity are also open sets, asymptotically approach χ [Lai & Grebogi,

2000b]. These inverse images of $\mathcal{O}$ are a subset of the tongue anchored at $x = \chi$. The set of tongues, off the symmetry plane $y = 0$, forms an open and dense set, while its complement is a closed Cantor set of positive measure [Grebogi *et al.*, 1985]. An initial condition very close to the invariant subspace at $y = 0$ generates a trajectory that wanders erratically back and forth in the x-direction, due to the large eigenvalue ($L_u = 2$) of the tangent map, until, if the trajectory is not already in the tongues, noise will push it in a tongue and it will asymptote to infinity [Grebogi *et al.*, 1983b]. Since just after the bifurcation these tongues may be very narrow, it might take a very large time for an orbit to enter a tongue and be ejected away [Viana & Grebogi, 2000].

As p is further increased past $p_c = 1$, many other unstable periodic orbits embedded in the chaotic set at $y = 0$ lose transversal stability, and more and more saddles become repellers. The relative proportion between saddles and repellers changes with varying p, in a way that can be quantitatively treated using the methods to be described in the following section.

6. Quantifying Unstable Dimension Variability

6.1. *Finite-time Lyapunov exponents*

The relative abundance of periodic orbits with a different number of unstable directions can be evaluated by calculating the corresponding finite-time Lyapunov exponents [Abarbanel *et al.*, 1991]. These are computed in the same way as is done for the commonly used Lyapunov exponents, but using a finite (and usually short) timespan $n < \infty$. Its use in nonlinear dynamics is receiving a growing interest, since many dynamical regimes can be identified by using them [Prasad & Ramaswamy, 1999].

It has been recognized as a fingerprint of UDV in dynamical systems — the fluctuating behavior (around zero) of the time-n exponent closest to zero [Dawson *et al.*, 1994]. To understand qualitatively why does it happen, for the example studied in the previous section, let us consider an initial condition off but very close to the invariant subspace Σ. The resulting trajectory is properly quoted as a chaotic transient, since it eventually goes to infinity. Before this occurs, however, this transient orbit visits ε-neighborhoods of saddles and repellers of the invariant set for any ε, *no matter how small*. This means that there are time-n segments for which the trajectory is transversely attracting (in average) and others for which it is transversely repelling (also in average). This is properly quantified by time-n Lyapunov exponents along the transversal y-direction.

In order to apply this concept to the previously studied example, we will present the definitions only for a N-dimensional map $\mathbf{f}(\mathbf{x})$, but they can be straightforwardly extended to continuous-time flows as well. Let n be a positive integer and $\mathbf{Df}^n(\mathbf{x}_0)$ be the Jacobian matrix of the n times iterated map, with entries evaluated at $\mathbf{x}_0$. Suppose that the singular values of $\mathbf{Df}^n(\mathbf{x}_0)$ are ordered: $\xi_1(\mathbf{x}_0, n) \geq \xi_2(\mathbf{x}_0, n) \geq \cdots \geq \xi_n(\mathbf{x}_0, n)$. Then, the kth time-n Lyapunov exponent for the point $\mathbf{x}_0$ is defined as [Kostelich *et al.*, 1997]

$$\lambda_k(x_0, y_0; n) = \frac{1}{n} \ln \|\mathbf{Df}^n(x_0, y_0).\mathbf{v}_k\| , \qquad (16)$$

where $\mathbf{v}_k$ is the singular vector related to $\xi_k(\mathbf{x}_0, n)$.

The infinite time-limit of the above expression is the usual Lyapunov exponent $\lambda_k = \lim_{n\to\infty} \lambda_k(\mathbf{x}_0, n)$. Although the time-$n$ exponent $\lambda_k(\mathbf{x}_0, n)$ generally takes on a different value, depending on the point we choose, the infinite time limit takes on the same value for almost all $\mathbf{x}_0$ with respect to the natural ergodic measure of the invariant set [Viana & Grebogi, 2001]. For the map studied in the previous section there are two such exponents,

$$\lambda_1(x_0, y_0; n) = \frac{1}{n} \sum_{i=1}^{n} \ln[a(1 - 2x_i)] , \qquad (17)$$

$$\lambda_2(x_0, y_0; n) = \frac{1}{n} \sum_{i=1}^{n} \ln \left[p e^{-b(x_i - \chi)^2} + 3y_i^2 \right] , \qquad (18)$$

and we focus our attention on the transversal one, $\lambda_2(x_0, y_0; n)$, which infinite time limit is the conditional Lyapunov exponent λ_T for the invariant set Ω. If λ_T goes through zero from negative values (a *blowout bifurcation* [Ashwin *et al.*, 1994]) the invariant set loses transversal stability. As p increases past $p_c = 1$, an increasing number of saddles in Ω lose transversal stability. We have described in detail this transition for a period-1 orbit (fixed point), but similar bifurcations — often named *bubbling bifurcations* [Ashwin *et al.*, 1996] — occur for other periodic orbits as p increases.

If Ω displays UDV, the time-n Lyapunov exponent in the transversal direction will erratically

fluctuate about zero, which suggests the use of a probability density $P_L(\lambda_2(x_0, y_0; n), n)$, so that $P_L(\lambda_2(n), n)d\lambda_2$ is the probability that the time-n exponent takes on a value between λ_2 and $\lambda_2 + d\lambda_2$ for a given n [Kostelich *et al.*, 1997]. The initial conditions (x_0, y_0) are randomly chosen according to the Lebesgue measure of Ω. From this probability distribution we can obtain moments of functions of the time-n exponent, as averages

$$\langle F(\lambda_2(\mathbf{x}_0, n))\rangle = \int_{-\infty}^{+\infty} F(\lambda_2(\mathbf{x}_0, n)) P_L(\lambda_2(\mathbf{x}_0, n), n) d\lambda_2 \,, \quad (19)$$

assuming proper normalization for $P_L(\lambda_2, n)$.

For n large enough the form of this distribution can be written in the following form [Ellis, 1985]

$$P_L(\lambda_2(n), n) \approx \sqrt{\frac{nG''(\lambda_T)}{2\pi}}\, e^{-nG(\lambda_2)} \,, \quad (20)$$

where λ_T is the infinite-time limit of $\lambda_2(n)$, and the function $G(\lambda)$ has the following properties:

$$G(\lambda_T) = G'(\lambda_T) = 0 \,, \quad G''(\lambda_T) > 0 \,. \quad (21)$$

Expanding $G(\lambda)$ in the vicinity of λ_T, the first non-vanishing term is the quadratic one, i.e. $P_L(\lambda_2)$ is expected to have a Gaussian shape

$$P_L(\lambda_2) \approx \sqrt{\frac{nG''(\lambda_T)}{2\pi}}\, \exp\left[-\frac{nG''(\lambda_T)}{2}\,(\lambda_2 - \lambda_T)^2\right], \quad (n \gg 1) \,. \quad (22)$$

We can obtain a numerical approximation for this probability distribution by considering a large number of trajectories of length n from initial conditions randomly chosen in the chaotic invariant set. In Fig. 4 we show some distributions of time-50 exponents, obtained for different values of the bifurcation parameter p. We see that their shape is indeed Gaussian, and the distribution as a whole drifts toward positive values of λ_2, as p increases. The rate in which this drift occurs is not constant, however, as it can be seen in Fig. 5, where the average value of the time-n exponents, $m = \langle\lambda_2(n)\rangle$, is plotted *versus* the bifurcation parameter p.

The variance of the average m, with respect to a sample of size n, which we denote σ_n^2, is a constant value about 0.035 for all p-values, indicating that the Gaussian nature of the distribution $P_L(\lambda_2)$ is not significantly altered. A standard result [Bulmer, 1979] says that the variance of the total population is equal to the product of the variance of the average by the sample size, hence the total variance of the time-n exponents is $\sigma^2 = n\sigma_n^2$, equal to 1.75 for the time-50 exponent distributions depicted in Fig. 4.

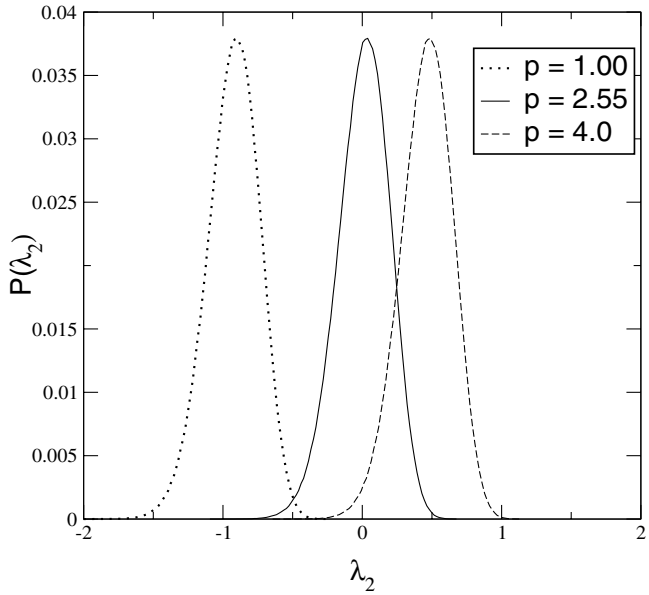

Fig. 4. Probability distribution $P(\lambda_2, 50)$ for time-50 transversal exponents and different values of the bifurcation parameter p. The remaining parameters are $a = 4.0$ and $b = 5.0$.

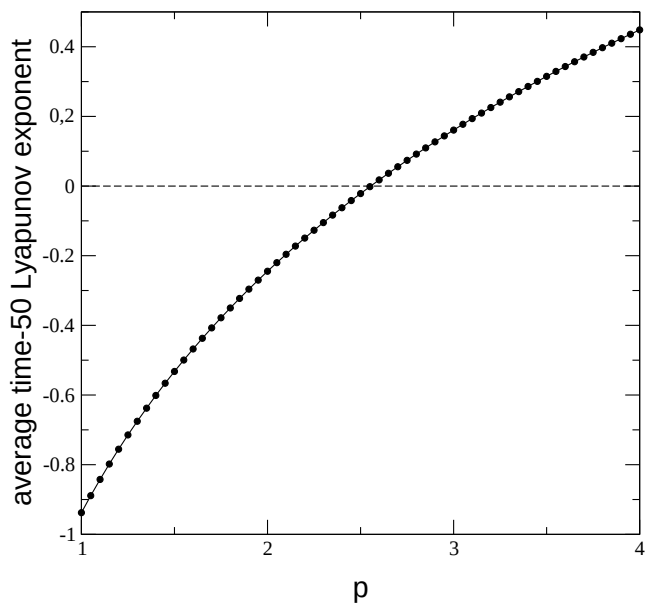

Fig. 5. Average transversal time-50 Lyapunov exponent as a function of p. Other parameters are the same as in the previous figure. It crosses the horizontal axis at $p^* \approx 2.55$, which signals a blowout bifurcation.

6.2. *Natural measure and unstable periodic orbits*

Although the fluctuating behavior of the time-n exponents has proven to be a useful diagnostic for the presence of UDV in a chaotic system, it is necessary to quantify the intensity of this effect, since it is apparent from the drifting behavior of $P_L(\lambda_2, 50)$ shown in Fig. 4 that, for increasing p, progressively more exponents become positive. This indicates that a growing number of periodic orbits embedded in the chaotic invariant set become transversely unstable. For $m \approx 0$ we would expect as many negative exponents as positive ones, and that situation would maximize the effect of UDV. Using arguments from the ergodic theory of chaotic sets, and a significant amount of previous numerical evidence, it follows that UDV is more pronounced when the infinite-time transversal Lyapunov exponent (λ_T) vanishes [Lai & Grebogi, 2000a].

To compute the conditional exponent λ_T we use typical trajectories on the chaotic invariant set Ω, with respect to its natural measure $\mu(\Omega)$. Since there are an infinite number of unstable periodic orbits embedded in Ω, they support the natural measure in the sense that, when computing λ_T, these periodic orbits contribute with different weights. These weights are determined by the natural measure of a typical trajectory which visits the neighborhoods of the periodic orbits, and are related to the magnitudes of the unstable eigenvalues of those unstable orbits [Lai & Grebogi, 2000a]. The natural measure of a typical trajectory in the neighborhood of a periodic orbit is related to the probability of being in its vicinity, and it is smaller for a more unstable periodic orbit [Farmer *et al.*, 1983]. Hence, the larger is the unstable eigenvalue of the periodic orbit, the smaller is its contribution to the natural measure. Summing over all unstable period-q orbits embedded in the invariant set Ω gives then its natural measure [Grebogi *et al.*, 1998b]

$$\mu(\Omega) = \lim_{q\to\infty} \sum_{\mathbf{x}_q(j)\in\Omega} \frac{1}{L_u(\mathbf{x}_q(j))}\,, \tag{23}$$

where $\mathbf{x}_q(j)$ is the jth fixed point of $\mathbf{f}^q(\mathbf{x})$, i.e. $\mathbf{x}_q(j)$ is on a period-r orbit, where r is q or a prime factor of q, and L_u is the expanding eigenvalue of this orbit. This expression was originally derived for hyperbolic systems [Grebogi *et al.*, 1998b], but its validity for nonhyperbolic ones has been verified in all analyzed cases [Lai *et al.*, 1997].

The natural measure associated with the jth period-q orbit is the normalized ratio [Lai & Grebogi, 2000a]

$$\mu_q(j) = \frac{1/L_u(\mathbf{x}_q(j), q)}{\sum_{\ell=1}^{N_q} [1/L_u(\mathbf{x}_q(\ell))]}\,, \tag{24}$$

where N_q is the number of period-q orbits. N_q^s and N_q^u are the numbers of transversely stable and unstable period-q orbits, respectively, such that $N_q^s + N_q^u = N_q$. In the case example of Sec. 5, when $q = 1$ it turns out that N_1^s and N_1^u are the numbers of saddles and repellers, respectively. The weights of the transversely stable and unstable period-q orbits are given, respectively, by

$$\Lambda_q^s = \sum_{j=1}^{N_q^s} \mu_q(j)\lambda_2(\mathbf{x}_q(j), q) \quad (\text{for } \lambda_2(\mathbf{x}_q(j), q) < 0)\,, \tag{25}$$

$$\Lambda_q^u = \sum_{j=1}^{N_q^u} \mu_q(j)\lambda_2(\mathbf{x}_q(j), q) \quad (\text{for } \lambda_2(\mathbf{x}_q(j), q) > 0)\,, \tag{26}$$

where $\lambda_2(\mathbf{x}_q(j), q)$ is the time-q transversal Lyapunov exponent for the jth period-q orbit. If $\lambda_2(\mathbf{x}_q(j), q)$ is positive (negative) the periodic orbit is transversely unstable (stable).

When λ_T becomes zero, at the blowout bifurcation point, it follows that the contributions of the transversely stable and unstable period-q orbits are exactly counterbalanced, and UDV is expected to be more intense. We can verify this prediction for the case example studied in the previous section, for it presents a variable bifurcation parameter p, such that, for $p > 1$, the system exhibits UDV. The infinite-time transversal Lyapunov exponent Λ_T vanishes for $p = p^* \approx 2.55$, which is the critical value for the blowout bifurcation.

A linear stability analysis indicates three qualitatively different regimes for Ω, according to the corresponding value of p:

(i) $0 < p < p_c = 1$: Ω is a chaotic attractor, in which all embedded unstable orbits are saddles, i.e. Ω is transversely stable as a whole. There is no UDV at all. $p = p_c$ is a saddle–repeller bifurcation point.

(ii) $p_c \le p < p^* \approx 2.55$: Ω is a chaotic saddle, in which there are "more" saddles than repellers,

in the sense that the natural measure is supported mainly by the transversely stable orbits. Ω is, on the average, transversely stable. The effect of UDV is progressively more intense as p increases from p_c. $p = p^*$ is a blowout bifurcation point.

(iii) $p \geq p^*$: Ω is still a chaotic saddle, but there are "more" repellers than saddles, in the same sense as before. Ω is, also on the average, transversely unstable.

Since, for $p > 1$, a trajectory off the invariant subspace eventually asymptotes to infinity, it would seem at first that Ω could not be transversely stable at all. However, our transversal stability analysis is linear, whereas the escaping of trajectories to infinity is a nonlinear effect [due to the cubic y^3 term in Eq. (15)]. Therefore, even though in case (ii) the chaotic saddle was found to be linearly transversely stable, it is nonlinearly transversely unstable, in the sense that any trajectory off the chaotic saddle eventually escapes to infinity.

From Eq. (22), the distribution of the transversal time-n exponents, $P_L(\lambda_2(n))$, is centered at $\lambda_2 = \lambda_T$, so that $m = \lambda_T$, which also follows from direct integration. Accordingly, the total variance is $\sigma^2 = n < (\lambda_2 - m)^2 >= 1/G''(\lambda_T)$, which is independent of n.

A quite direct procedure to quantify the relative abundance of saddles and repellers in the chaotic invariant set Ω is to compute the fraction of positive transversal time-n exponents [Viana & Grebogi, 2001]

$$\phi(n) = \int_0^\infty P_L(\lambda_2(\mathbf{x}_0, n), n) d\lambda_2 \qquad (27)$$

shown in Fig. 6 as a function of p. For $p < 1$ it is zero and increases monotonically for $p \geq 1$, saturating at $\phi = 1$ for large p. At the blowout bifurcation point p^* we have $\phi = 1/2$, for exactly half of the time-n exponents that are positive. Using the asymptotic expression of $P_L(\lambda_2, n)$ there results

$$\phi(n) = \frac{1}{2} + \frac{\sqrt{\pi}}{2} \operatorname{erf}\left(\lambda_T \sqrt{\frac{nG''(\lambda_T)}{2}}\right), \qquad (28)$$

in complete agreement with the numerical result.

7. UDV-Induced Intermittency

In this section, we will slightly modify the map introduced in Sec. 5 by changing the sign of the cubic term, which introduces a fold in the map dynamics

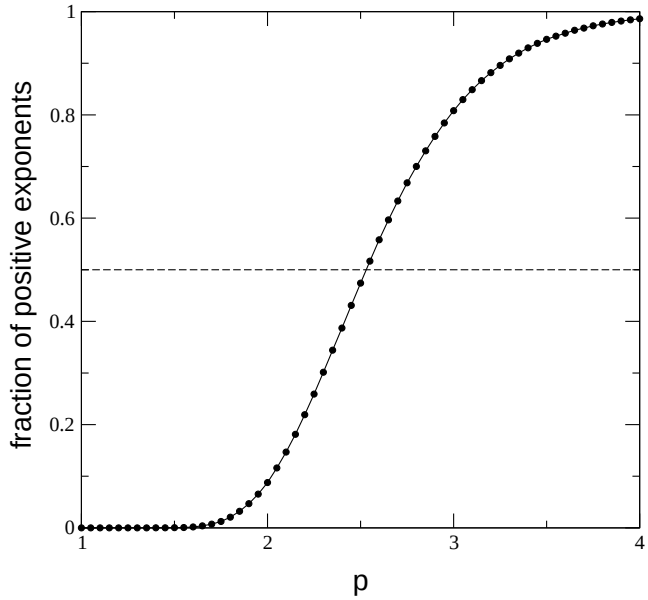

Fig. 6. Fraction of positive time-50 transversal Lyapunov exponents as a function of p, for the same parameters as in the previous figures.

along the transversal direction. This does not affect the results of the linear stability analysis, but prevents trajectories from escaping to infinity. Hence, trajectories starting off but very close to the invariant subspace $y = 0$ spend large amounts of time near $y = 0$ before being ejected away, in the form of intermittent chaotic bursts. We can call the process *UDV-induced intermittency*, since here chaotic bursting is accompanied by the lack of hyperbolicity (Sauer [2002] has called UDV an "intermittency in miniature").

In order to describe the onset and evolution of such intermittency in the map described in Sec. 5, we consider a reference, or "true" chaotic trajectory in the invariant set $\Omega \subset \mathcal{M}$. However, the existence of the invariant subspace $\mathcal{M}$ is jeopardized by the lack of model symmetry caused by small, yet unavoidable imperfect parameter determination, and extrinsic noise. We thus expect that a computer-generated trajectory thought to belong to $\mathcal{M}$ will actually start off but very close to $\mathcal{M}$. The shadowing distance between the "true" chaotic trajectory at $\mathcal{M}$ and the pseudo-trajectory initialized nearby is, at each instant, the pointwise distance between them in the phase plane. The existence of laminar intervals, for which the pseudo-trajectory is close to $\mathcal{M}$, is equivalent to having a pseudo-trajectory which continuously shadows the "true" chaotic trajectory belonging to $\mathcal{M}$. By the same

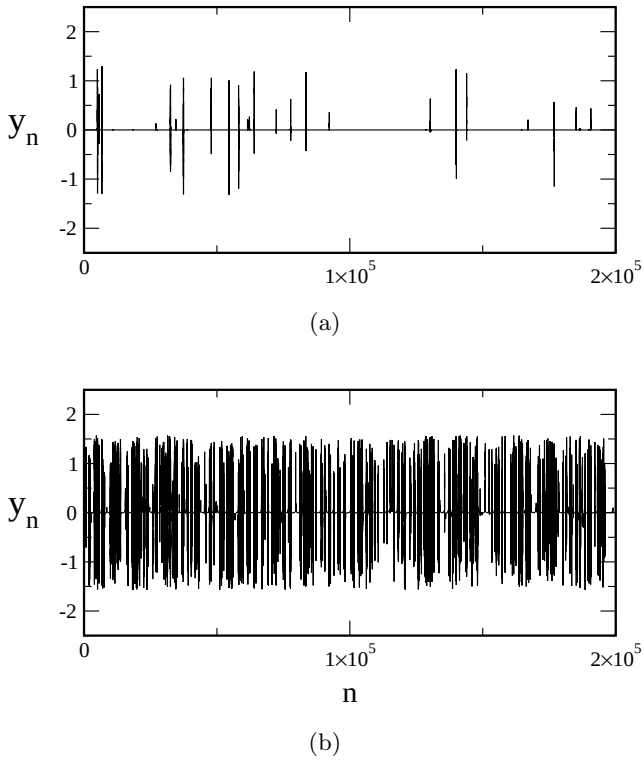

Fig. 7. Pseudo-trajectories generated for the map (14)–(15) with $a = 4.0$, $b = 5.0$, and a noise level 10^{-q}, with $q = 16$, and (a) $p = 2.30$; (b) $p = 2.55$.

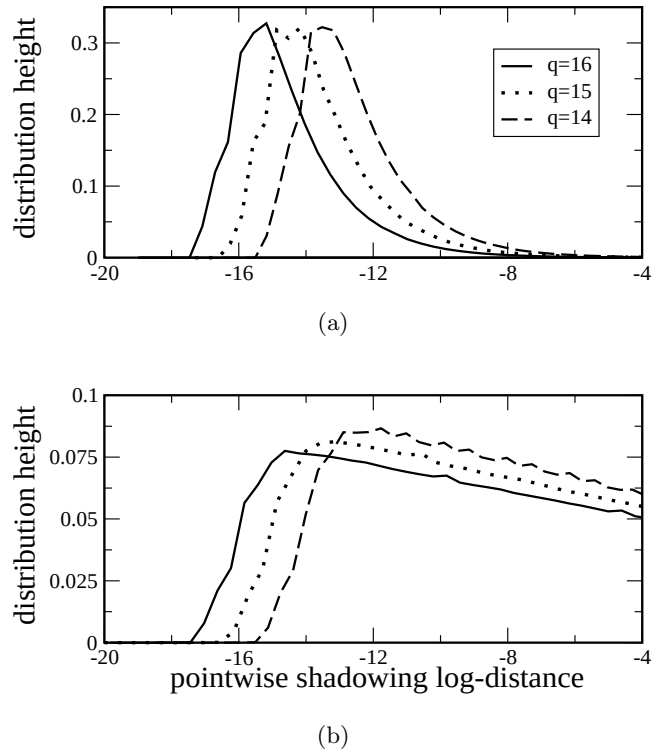

Fig. 8. Statistical distribution of pointwise shadowing log-distances for (a) $p = 2.10$, (b) $p = 2.55$, and three different noise levels.

token, bursting is an observable manifestation of the lack of shadowability, while the lengths of the laminar intervals yield estimates for shadowing times. Hence, the properties of chaotic bursting are related to the statistics of shadowing distances and times.

A "true" chaotic trajectory is known to exist for initial trajectories $(x_0, y_0 = 0)$ randomly chosen in Ω with respect to the Lebesgue measure. The pseudo-trajectories we generate are meant to represent numerically obtained orbits, for which we cannot have initial conditions exactly placed at $y = 0$, in that they have some uncertainty in the transversal direction. Since the x-part of the map (14) does not depend on y, the evolution along the x-direction of both trajectories is the same for all times, and the pointwise distance between a chaotic trajectory and a pseudo-trajectory will be simply the value of y_n for the latter. Finally, a computer generated pseudo-trajectory is likely to suffer the action of round-off errors, which we can simulate by corrupting a pseudo-trajectory with randomly applied kicks of small magnitude 10^{-q}, playing the role of one-step errors [Sauer, 2002].

We must emphasize that the pseudo-trajectories do not belong to Ω but, instead, to a larger invariant set of which Ω is a subset. The fold introduced in the y-part of the map (15) ensures that this larger chaotic set is recurrently close to $\mathcal{M}$ and does not asymptote to infinity, as it would be the case if the cubic term in (15) would have a positive sign. In Fig. 7, we show two examples of high-precision pseudo-trajectories generated using the procedure described above. The noise level is fixed at 10^{-16}, which can be regarded as the computer roundoff introduced by a double precision floating-point arithmetics. Figures 7(a) and 7(b) refer to different post-critical values of the bifurcation parameter ($p > 1$). We record the values of y_n, or the pointwise shadowing distances, at each time, yielding the corresponding log-distances $z_n = \ln |y_n|$. The use of an external kick creates a "barrier" of width 10^{-q} preventing pseudo-trajectories from having shadowing log-distances less than $-q$ on average. The shadowing distances may be large due to chaotic bursting, but they are predominantly very small (within the laminar regions); the bursting being more effective as p increases.

Figure 8 presents numerically obtained statistical distributions of the shadowing log-distances z_n for two post-critical values of p and external kicks

of different magnitudes. In all depicted cases, the (normalized) distribution height falls rapidly down to zero for shadowing distances less than 10^{-q}, as expected, and decreases exponentially for higher shadowing distances

$$P_d(z) = P_{d0} \exp[-\kappa(p)(z - \ln q)] , \qquad (29)$$

where $P_d(z)dz$ is the probability for the shadowing log-distance to lie between z and $z + dz$. As p increases from 2.10 [Fig. 8(a)] to 2.55 [Fig. 8(b)] this decrease becomes slower, meaning that, as the UDV effect is more intense, we have a progressive dominance of higher shadowing distances. This is in accordance with the greater content of transversely unstable periodic orbits as p is increased from $p_c = 1$.

The shadowing log-distances experience spikes of various heights, but remain in the immediate vicinity of the invariant subspace $\mathcal{M}$, until they burst chaotically and return to $\mathcal{M}$. We define the shadowability time as the interval it takes for the pointwise shadowability distance to grow to the order of the attractor size, say $y = y_A = 1$. Figure 9 shows the dependence of the log-shadowing times, for different values of p, on the noisy kick strength level q. The results suggest that the distribution of the average shadowing times has a power-law scaling with respect to the noise level q, what can also be derived by integrating the distribution (29) for shadowing log-distances, in order to obtain the probability for a shadowing distance to be greater than y_A, such that $P_t(q) \sim \exp[-\kappa(p)(\ln y_A - \ln q)] = q^{\kappa(p)}$.

These probability distributions for the shadowing distances and times can be theoretically justified from the statistical properties of finite-time Lyapunov exponents. A pseudo-trajectory starting off but near the invariant subspace will wander along the x-direction according to the unstable eigenvalue of the periodic orbits embedded in Ω. As the trajectory approaches orbits with different numbers of unstable direction, it will move either toward or apart from Ω for finite time segments. Let y_k be the shadowing distance of the pseudo-trajectory at time k. During a short time interval of length n, the local expansion rate is the corresponding time-n transversal exponent, such that $y_{k+n} \sim y_k \exp(n\lambda_2(n))$. It follows that the log-shadowing distances satisfy $z_{k+n} \sim z_k + n\lambda_2(n)$.

When Ω exhibits UDV, the time-n exponents $\lambda_2(n)$ fluctuate in an irregular fashion about zero, being the random innovations which push the log-shadowing distances toward or away from the chaotic trajectory confined to the invariant subspace $\mathcal{M}$. The time evolution of the log-shadowing distances can thus be regarded as an additive random process, with a diffusion rate being given by the dispersion of the time-n exponents, which we have measured by the total variance σ^2 of their statistical distribution $P_L(\lambda_2(n), n)$. However, the distribution of $\lambda_2(n)$ is such that there is a different amount of positive and negative values (see Fig. 4). For example, if their average m is positive the transversal displacements of a pseudo-trajectory will have a positive average expansion rate, which describes a biased random walk, in which a drift m has been included [Sauer *et al.*, 1997].

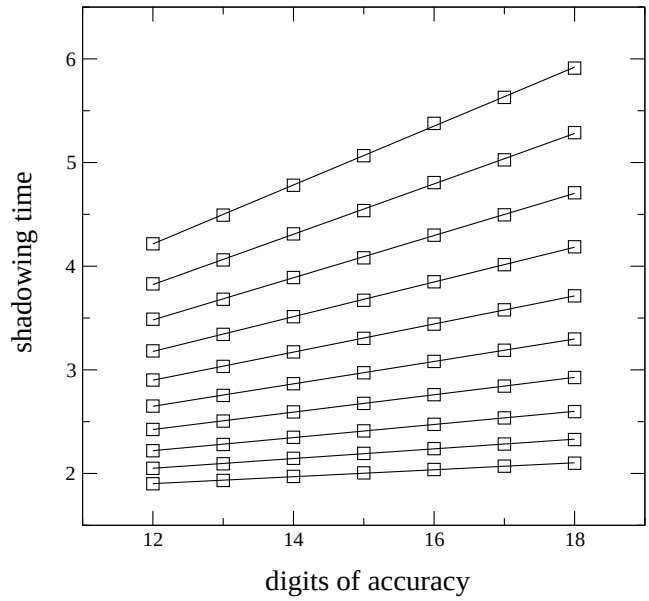

Fig. 9. Shadowing times as a function of the kick strength exponent, or the number of accuracy digits. The various lines are least-squares fits obtained for different values of the bifurcation parameter p. The top line is for $p = 2.1$ and the lines below are for values of p with a constant increment of $\delta p = 0.05$. The slopes of these lines are depicted as boxes in Fig. 10.

A diffusion equation describes the spatio-temporal evolution of the distribution of the shadowing log-distances $\mathcal{P}(z, n)$ with respect to the time-n and the log-distance z (assumed to be continuous variables) [Feller, 1957]:

$$\frac{\partial \mathcal{P}(z,n)}{\partial n} = \frac{\sigma^2}{2} \frac{\partial^2 \mathcal{P}(z,n)}{\partial z^2} + m \frac{\partial \mathcal{P}(z,n)}{\partial z} . \qquad (30)$$

The effect of the kicks added to the pseudo-trajectories can be included in this stochastic model

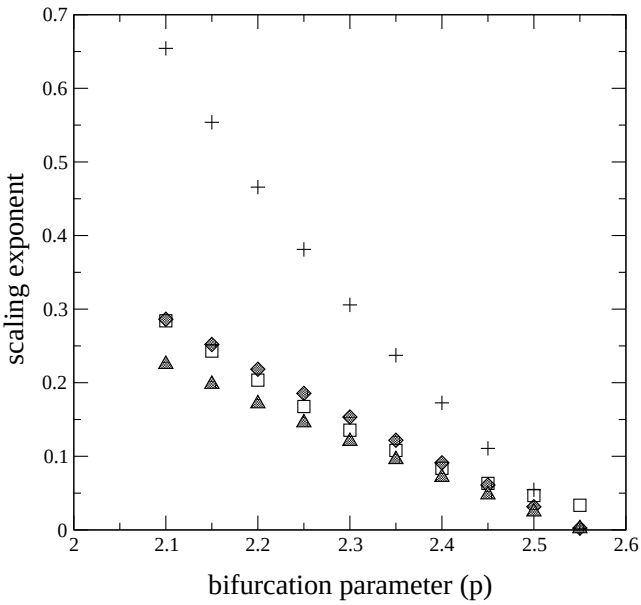

Fig. 10. Comparison between the slopes of statistical distributions of shadowing log-distances and times. The numerically obtained slopes for distributions of log-shadowing distances (crosses) are based on Fig. 9; diamonds (triangles) stand for the theoretical prediction of Eq. (31), based on time-2 (time-50) Lyapunov exponents; boxes are for numerically obtained distribution slopes of shadowing times, according to Fig. 9.

by including a reflecting barrier at $z^* \sim -q$. Moreover, we impose the following boundary conditions: $\mathcal{P}(z \to \infty) = (\partial \mathcal{P}/\partial z)_{z\to\infty} = 0$.

The diffusion process governed by Eq. (30) has an equilibrium distribution given by $(\partial \mathcal{P}_{EQ}/\partial n) = 0$, which reads [Pinto *et al.*, 2002]

$$\mathcal{P}_{EQ}(z) = \frac{2|m|}{\sigma^2} \exp\left[-\frac{2|m|}{\sigma^2}(z - \ln\, q)\right], \qquad (31)$$

which is similar to the numerically obtained distribution $P_d(z)$, given by Eq. (29), if we identify the decay exponent κ with the so-called *hyperbolicity exponent* [Sauer, 2002]

$$h \equiv \frac{2|m|}{\sigma^2}. \qquad (32)$$

Figure 10 shows a comparison between the numerically obtained slopes of the exponentially decaying distributions (crosses) and the theoretical prediction of Eq. (32) (diamonds and triangles are for different time-n exponents). There is an increasingly better agreement among these values, as we approach $p = p^* = 2.55$, the value for which the UDV effect is more pronounced. The good agreement between theory and numerical experiment at $p = p^*$ is a consequence of the fact that, when UDV is more intense, the average time-n exponent vanishes, such that there is an approximately equal number of positive and negative innovations acting on a pseudo-trajectory. In this case a Markovian random walk would be a better approximation of the actual behavior of the pseudo-trajectory under random kicks. As we move away from p^*, the bias caused by a nonzero average exponent makes the equilibrium distribution given by (31) a poorer version of the stochastic process. Actually the bursting is chaotic, and some degree of dynamical correlation is expected to take place at every moment, preventing us from successfully using linear stochastic models such as those considered here.

The time-2 exponent (shown as diamonds in Fig. 10) are consistently better than the time-50 ones (depicted as triangles in Fig. 10), which implies that the underlying dynamical structure causing UDV is actually very complicated. The saddles and repellers belonging to Ω are so densely intertwined that a pseudo-trajectory will have a different number of unstable directions over very short periods of time, and a time-2 exponent is expected to give results closer to a Markovian stochastic process, when compared with a time-50 exponent.

The stochastic model we use for a biased random walk with reflecting barrier can also be used to estimate the shadowing time τ, by imposing that $y_{n+\tau}$ be greater than $y_A = 1$. Using Laplace transforms, we can obtain the following theoretical estimate of the average shadowing time [Sauer *et al.*, 1997]

$$\langle \tau \rangle = \frac{1}{h}(q^h - 1) - \frac{\ln\, q}{|m|}. \qquad (33)$$

Since the statistical distribution of shadowing times scales linearly with τ, if q is small enough, Eq. (33) leads to an algebraic scaling with the noise level q, in agreement with the numerical result, provided the slope, once again, equals the hyperbolicity exponent h.

The slopes of the various curves in Fig. 9, corresponding to different values of the bifurcation parameter p, are depicted as boxes in Fig. 10. We have a better agreement between theoretical and numerical results for the shadowing times than for the log-distances. A plausible explanation for that is the different definitions we have used for shadowing distances and times. Whereas the former are precisely defined as pointwise distances between two trajectories, shadowing times, on the other hand,

are defined in a less accurate way since: (i) the times are measured when the log-distances exceed an arbitrary threshold; (ii) we compute average values over very long chaotic transients. Hence, the overall statistical behavior of shadowing times would be more likely emulated by a stochastic model.

To conclude this section, we have shown that, when a system fails to be hyperbolic due to UDV, it may present intermittent bursting if it exhibits some symmetry leading to a low-dimensional invariant subspace. This type of intermittent transition has been observed, for example, in the transition between synchronized and nonsynchronized behavior in a lattice of piecewise linear maps with a long-range coupling [Batista *et al.*, 2002]. For general systems of N coupled maps or oscillators, the invariant subspace of interest is the M-dimensional synchronization manifold (where $M \ll N$). UDV-induced intermittency in such complex systems would be explained by studying the stability of the synchronization manifold with respect to the corresponding $N - M$ transversal directions.

8. Conclusions

Unstable dimension variability (UDV) is a dynamical property of strongly nonhyperbolic invariant chaotic sets. Its consequences on the shadowability properties are severe, limiting in a dramatic way the use of single pseudo-trajectories to numerical computations of physically relevant quantities. Hence, these pseudo-trajectories can at best give the same kind of information furnished by a stochastic model, even though the governing dynamical equations are strictly deterministic. This is the reason we are calling them pseudo-deterministic systems. We reviewed previous work on UDV, which typically shows up in high-dimensional systems like coupled map or oscillator lattices, for which the invariant set of interest is the synchronization manifold. Hence UDV is far from being just a mathematical curiosity, likely to be found only in pathological dynamical systems. We thus expect severe shadowability problems in mathematical models of high-dimensional chaotic systems used in science and technology. This problem is even more pervasive if we note that most numerical integration schemes for partial differential equations rely on some kind of space and time discretization leading to such coupled systems.

This paper has focused on a simple dynamical model consisting of a two-dimensional noninvertible mapping with an invariant subspace, for two basic reasons. First, for such a system, the mathematical mechanism beneath the onset of UDV can be readily identified — a saddle–repeller bifurcation. Second, the system has a control parameter that enables us to quantify the intensity of the shadowing breakdown produced by UDV. By a combination of numerical and analytical arguments we identify the situation in which UDV is most severe: the blowout bifurcation point, where the invariant subspace loses transversal stability and half of the finite-time transversal exponents are positive. This enables us to estimate shadowing distances and times, according to a stochastic model of a biased random walk with reflecting barrier.

Acknowledgments

This work was made possible through partial financial support from the following Brazilian research agencies: FAPESP, CNPq, Fundação Araucária (Paraná) and FUNPAR (UFPR). We acknowledge enlightening discussions and useful comments by M. Baptista, E. Barreto, Y.-C. Lai, E. Macau, T. Sauer, P. So and J. Kurths.

References

Abarbanel, H. D. I., Brown, R. & Kennel, M. B. [1991] "Variation of Lyapunov exponents on a strange attractor," *J. Nonlin. Sci.* **1**, 175–199.

Abraham, R. & Smale, S. [1970] "Nongenericity of Ω-stability, global analysis I," *Proc. Symp. Pure Math. (AMS)* **14**, 5–8.

Andrade, V. & Lai, Y.-C. [2001] "Super persistent chaotic transients in physical systems: Effect of noise on phase synchronization of coupled chaotic oscillators," *Int. J. Bifurcation and Chaos* **11**, 2607–2619.

Anosov, D. V. [1967] "Geodesic flows and closed Riemannian manifolds with negative curvature," *Proc. Steklov Inst. Math.* **90**, 1.

Arnold, V. I. [1978] *Ordinary Differential Equations* (The MIT Press, Cambridge, MA).

Ashwin, P., Buescu, J. & Stewart, I. [1994] "Bubbling of attractors and synchronization of chaotic oscillators," *Phys. Lett.* **A193**, 126.

Ashwin, P., Buescu, J. & Stewart, I. [1996] "From attractor to chaotic saddle: A tale of transverse stability," *Nonlinearity* **9**, 703–737.

Barreto, E., So, P., Gluckman, B. J. & Schiff, S. J. [2000] "From generalized synchrony to topological decoherence: Emergent sets in coupled chaotic systems," *Phys. Rev. Lett.* **84**, 1689–1692.

Barreto, E. & So, P. [2000] "Mechanisms for the development of unstable dimension variability and the breakdown of shadowing in coupled chaotic systems," *Phys. Rev. Lett.* **85**, 2490–2493.

Batista, A. M., Pinto S. E. S., Viana, R. L. & Lopes, S. R. [2002] "Lyapunov spectrum and synchronization of piecewise linear map lattices with power-law coupling," *Phys. Rev.* **E65**, 056209.

Benedicks, M. & Carleson, L. [1991] "The dynamics of the Hénon map," *Ann. Math.* **133**, 73–169.

Boccaletti, S., Pecora, L. M. & Pelaez, A. [2001] "Unifying framework for synchronization of coupled dynamical systems," *Phys. Rev.* **E63**, 066219.

Bonatti, S. P. da C., Diaz, L. C. & Turcat, G. [2000] "Pas de 'shadowing lemma' pour les dynamiques partiellment hyperboliques," *C. R. Acad. Sci. Paris* **330**, 587–592.

Bowen, R. [1975] "ω-limit sets for axiom A diffeomorphisms," *J. Diff. Eq.* **18**, 333–339.

Bulmer, M. G. [1979] *Principles of Statistics* (Dover, NY).

Davidchack, R. & Lai, Y.-C. [2000] "Characterization of transition to chaos with multiple positive Lyapunov exponents by unstable periodic orbits," *Phys. Lett.* **A270**, 308–313.

Dawson, S. P., Grebogi, C., Sauer, T. & Yorke, J. A. [1994] "Obstructions to shadowing when a Lyapunov exponent fluctuates about zero," *Phys. Rev. Lett.* **73**, 1927–1930.

Dawson, S. P. [1996] "Strange nonattracting chaotic sets, crises, and fluctuating Lyapunov exponents," *Phys. Rev. Lett.* **76**, 4348–4351.

Devaney, R. L. [1989] *An Introduction to Chaotic Dynamical Systems* (Addison-Wesley, Reading).

Ellis, R. S. [1985] *Entropy, Large Deviations and Statistical Mechanics* (Springer-Verlag, NY).

Farmer, J. D., Ott, E. & Yorke, J. A. [1983] "The dimension of chaotic attractors," *Physica* **D7**, 153–180.

Feller, W. [1957] *An Introduction to Probability Theory and Its Applications*, Vol. I (Wiley, NY).

Grassberger, P., Badii, R. & Politi, A. [1989] "Scaling laws for invariant-measures on hyperbolic and nonhyperbolic attractors," *J. Stat. Phys.* **51**, 135–178.

Grebogi, C., Ott, E. & Yorke, J. A. [1983a] "Crises, sudden changes in chaotic attractors, and transient chaos," *Physica* **D7**, 181–200.

Grebogi, C., Ott, E. & Yorke, J. A. [1983b] "Fractal basin boundaries, long-lived chaotic transients, and unstable-unstable pair bifurcation," *Phys. Rev. Lett.* **50**, 935–938.

Grebogi, C., McDonald, S. W., Ott, E. & Yorke, J. A. [1985] "The exterior dimension of fat fractals," *Phys. Lett.* **A110**, 1–4.

Grebogi, C., Hammel, S. & Yorke, J. A. [1987] "Do numerical orbits of chaotic dynamical processes represent true orbits?" *J. Complexity* **3**, 136–145.

Grebogi, C., Hammel, S. & Yorke, J. A. [1988a] "Numerical orbits of chaotic processes represent true orbits," *Bull. Am. Math. Soc.* **19**, 465–470.

Grebogi, C., Ott, E. & Yorke, J. A. [1988b] "Unstable periodic orbits and the dimensions of multifractal chaotic attractors," *Phys. Rev.* **E37**, 1711–1724.

Grebogi, C., Hammel, S., Yorke, J. A. & Sauer, T. [1990] "Shadowing of physical trajectories in chaotic dynamics: Containment and refinement," *Phys. Rev. Lett.* **65**, 1527–1530.

Grebogi, C., Poon, L., Sauer, T., Yorke, J. A. & Auerbach, D. [2002] "Shadowability of chaotic dynamical systems," in *Handbook of Dynamical Systems*, ed. B. Fiedler (Elsevier, Amsterdam), Vol. 2, Chap. 7.

Guckenheimer, J. & Holmes, P. J. [1983] *Nonlinear Oscillations, Dynamical Systems, and Bifurcations of Vector Fields* (Springer-Verlag, NY).

Gulick, D. [1990] *Directions in Chaos* (McGraw Hill, NY).

Jacobson, M. V. [1981] "Absolutely continuous invariant measures for one-parameter families of one-dimensional maps," *Commun. Math. Phys.* **81**, 39–88.

Kantz, H., Grebogi, C., Prasad, A., Lai, Y.-C. & Sinde, E. [2002] "Unexpected robustness against noise of a class of nonhyperbolic chaotic attractors," *Phys. Rev.* **E65**, 026209.

Katok, A. & Hasselblatt, B. [1995] *Introduction to the Modern Theory of Dynamical Systems* (Cambridge University Press, Cambridge).

Kostelich, E. J., Kan, I., Grebogi, C., Ott, E. & Yorke, J. A. [1997] "Unstable dimension variability: A source of nonhyperbolicity in chaotic systems," *Physica* **D109**, 81–90.

Lai, Y.-C. [1996] "Unstable dimension variability and complexity in chaotic systems," *Phys. Rev.* **E59**, R3807–R3810.

Lai, Y.-C., Grebogi, C., Yorke, J. A. & Venkataramani, S. C. [1996] "Riddling bifurcation in chaotic dynamical systems," *Phys. Rev. Lett.* **77**, 55–58.

Lai, Y.-C., Nagai, Y. & Grebogi, C. [1997] "Characterization of the natural measure by unstable periodic orbits in chaotic attractors," *Phys. Rev. Lett.* **79**, 649–652.

Lai, Y.-C. & Grebogi, C. [1999] "Modeling of coupled chaotic oscillators," *Phys. Rev. Lett.* **82**, 4803–4806.

Lai, Y.-C., Grebogi, C. & Kurths, J. [1999a] "Modeling of deterministic chaotic systems," *Phys. Rev.* **E59**, 2907–2910.

Lai, Y.-C., Lerner, D., Williams, K. & Grebogi, C. [1999b] "Unstable dimension variability in coupled chaotic systems," *Phys. Rev.* **E60**, 5445–5454.

Lai, Y.-C. & Grebogi, C. [2000a] "Obstruction to deterministic modeling of chaotic systems with invariant subspace," *Int. J. Bifurcation and Chaos* **10**, 683–693.

Lai, Y.-C. & Grebogi, C. [2000b] "Riddling in dynamical systems," *EQUADIFF 99* (World Scientific, Singapore).

Lai, Y.-C., Liu, Z. H., Billings, L. & Schwartz, I. B. [2003] "Noise-induced unstable dimension variability and transition to chaos in random dynamical systems," *Phys. Rev.* **E67**, 026210.

Meyer, K. & Hall, G. R. [1992] *Introduction to Hamiltonian Dynamical Systems and the N-body Problem* (Springer, NY).

Palis, J. & de Melo, W. [1982] *Geometric Theory of Dynamical Systems: An Introduction* (Springer-Verlag, NY).

Pecora, L. M. & Carroll, T. L. [1990] "Synchronization in chaotic systems," *Phys. Rev. Lett.* **64**, 821–824.

Pinto, S. E. S., Viana, R. L. & Grebogi, C. [2002] "Chaotic bursting at the onset of unstable dimension variability," *Phys. Rev.* **E66**, 046213.

Poon, L., Dawson, S. P., Grebogi, C., Sauer, T. & Yorke, J. A. [1994] "Shadowing in chaotic systems," in *Dynamical Systems and Chaos*, eds. Aizawa, Y., Saito, S. & Shiraiwa, K. (World Scientific, Singapore), p. 13.

Prasad, A. & Ramaswamy, R. [1999] "Characteristic distributions of finite-time Lyapunov exponents," *Phys. Rev.* **E60**, 2761.

Romeiras, F. J., Grebogi, C., Ott, E. & Dayawansa, W. P. [1992] "Controlling chaotic dynamic systems," *Physica* **D58**, 165–192.

Ruelle, D. [1989] *Chaotic Evolution and Strange Attractors* (Cambridge University Press, Cambridge).

Sauer, T. & Yorke, J. A. [1991] "Rigorous verification of trajectories for the computer simulation of dynamic systems," *Nonlinearity* **4**, p. 961.

Sauer, T., Grebogi, C. & Yorke, J. A. [1997] "How long do numerical chaotic solutions remain valid?" *Phys. Rev. Lett.* **79**, 59–62.

Sauer, T. [2002] "Shadowing breakdown and large errors in dynamical simulations of physical systems," *Phys. Rev.* **E65**, 036220.

Viana, R. L. & Grebogi, C. [2000] "Unstable dimension variability and synchronization of chaotic systems," *Phys. Rev.* **E62**, 462–468.

Viana, R. L. & Grebogi, C. [2001] "Riddled basins and unstable dimension variability in chaotic systems with and without symmetry," *Int. J. Bifurcation and Chaos* **11**, 2689–2698.

Wiggins, S. [1990] *Introduction to Applied Nonlinear Dynamical Systems and Chaos* (Springer-Verlag, NY).